



HAL
open science

Absorptive nature of scattering coefficients in stress-energy tensor formalism for room acoustics

Jean-Dominique Polack, Hugo Dujourdy, Roland Badeau

► **To cite this version:**

Jean-Dominique Polack, Hugo Dujourdy, Roland Badeau. Absorptive nature of scattering coefficients in stress-energy tensor formalism for room acoustics. *Journal of the Acoustical Society of America*, 2024, 155 (4), pp.2339 - 2346. 10.1121/10.0025468 . hal-04548715v2

HAL Id: hal-04548715

<https://telecom-paris.hal.science/hal-04548715v2>

Submitted on 23 Aug 2024

HAL is a multi-disciplinary open access archive for the deposit and dissemination of scientific research documents, whether they are published or not. The documents may come from teaching and research institutions in France or abroad, or from public or private research centers.

L'archive ouverte pluridisciplinaire **HAL**, est destinée au dépôt et à la diffusion de documents scientifiques de niveau recherche, publiés ou non, émanant des établissements d'enseignement et de recherche français ou étrangers, des laboratoires publics ou privés.

Absorptive nature of scattering coefficients in stress-energy tensor formalism for room acoustics

Jean-Dominique Polack,¹ Hugo Dujourdy,² and Roland Badeau³

¹*Sorbonne Université, CNRS UMR 7190, Institut Jean le Rond d'Alembert, F-75005 Paris, France*

²*Diffusion Acoustic, F-92150 Suresnes, France*

³*LTCI, Télécom Paris, F-91120 Palaiseau, France^a*

(Dated: 28 February 2024)

1 In the stress-energy tensor formalism, the symmetry between absorption and scatter-
2 ing coefficients, as proven by measurements combined with simulations, is counter-
3 intuitive. By introducing the wall admittance, we show that the scattering coefficient
4 is partly created by the real part of the wall admittance combined with the active
5 intensity, that is, is partly due to absorption. However, for curved surfaces or finite
6 source distances, it also depends on the imaginary part of the wall admittance in
7 combination with the reactive intensity, which confers it genuine scattering proper-
8 ties inversely proportional to the distances to the sources. Thus, for plane waves
9 impinging on plane boundaries, or purely real admittances, scattering reduces to
10 absorption.

^a)jean-dominique.polack@sorbonne-universite.fr

11 I. INTRODUCTION

12 The stress-energy tensor formalism was initially introduced by Morse and collaborators
13 (Morse and Feshbach, 1956; Morse and Ingard, 1968) in order to describe energy conservation
14 in linear acoustics. Many years later, Stanzial and collaborators applied the conservation
15 of the stress-energy tensor to room acoustics (Stanzial *et al.*, 2002), focusing on the expres-
16 sion of the radiation pressure. In a subsequent paper (Stanzial and Schiffrer, 2010), they
17 introduced the energy velocity as ratio of the sound intensity to the total acoustic energy,
18 and derived from the conservation of the stress-energy tensor an expression for the local
19 initial reverberation time at the onset of energy decay. Some related ideas, linking wave
20 impedance to the complex sound intensity, are also found in (Mann *et al.*, 1987; Stanzial
21 and Graffigna, 2017). Mann *et al.* focused on energy transfer and analysed in terms of
22 energy flux and power what happens in the vicinity of intensity vortex that are created
23 by specific configurations of sources. Stanzial and Graffigna went one step further in the
24 definition and measurement of complex intensity. However, both papers are outside the
25 scope of the present analysis that focuses on the active stress-energy tensor - see (Polack,
26 2023) for an extension to the *complex* stress-energy tensor and its conservation, together
27 with preliminary measurement results.

28 A somewhat different perspective was introduced by Dujourdy *et al.* (Dujourdy *et al.*,
29 2017; 2019) in order to generalize the diffusion equation formalism of Ollendorf and Picaut
30 (Ollendorff, 1969; Picaut *et al.*, 1997). Indeed, where the diffusion equation arbitrarily
31 introduces a gradient type relationship between sound intensity and total energy, the stress-

32 energy tensor formalism introduces instead the conservation equation for intensity. When
 33 integrated in disproportionate enclosures, the stress-energy tensor yields both absorption
 34 and scattering on the boundaries. Dujourdy *et al.* stressed the symmetrical role played
 35 by absorption and scattering coefficients in the conservation equations, which was then
 36 systematically investigated and confirmed by Meacham *et al.* (Meacham *et al.*, 2019). The
 37 present papers aims at proving this symmetry and the absorbing nature of the scattering
 38 coefficient, using the local admittance formalism at the boundaries.

39 After presenting the background of the stress-energy conservation, we successively express
 40 the elements of the stress energy tensor on the boundaries, then the absorption and scattering
 41 coefficients, in terms of the local admittance. We then examine the main types of boundaries,
 42 and discuss the relationship between absorption and scattering coefficients.

43 II. THE BASIC EQUATIONS

44 Dujourdy *et al.* (Dujourdy *et al.*, 2017, 2019) have shown that the wave equation, satisfied
 45 by the velocity potential, can be extended by a set of conservation equations that reduces
 46 to the conservation of the stress-energy tensor \underline{T} .

47 Let ψ be the velocity potential. The conservation of the stress-energy tensor is expressed
 48 as:

$$\vec{\nabla} \cdot \underline{T} = 0 \tag{1}$$

49 with

$$\underline{\underline{T}} = \begin{pmatrix} E_{tt} & E_{tx} & E_{ty} & E_{tz} \\ E_{tx} & E_{xx} & E_{xy} & E_{xz} \\ E_{ty} & E_{xy} & E_{yy} & E_{yz} \\ E_{tz} & E_{xz} & E_{yz} & E_{zz} \end{pmatrix}$$

50 In terms of the velocity potential, the elements of the stress-energy tensor are given by:

$$E_{tt} = \frac{\rho}{2} \left(\frac{1}{c^2} |\partial_t \psi|^2 + |\vec{\nabla} \psi|^2 \right)$$

$$E_{tx} = -\frac{\rho_0}{c} \partial_t \psi \partial_x \psi$$

$$E_{ty} = -\frac{\rho_0}{c} \partial_t \psi \partial_y \psi$$

$$E_{tz} = -\frac{\rho_0}{c} \partial_t \psi \partial_z \psi$$

$$E_{xx} = \frac{\rho_0}{2} \left(\frac{1}{c^2} |\partial_t \psi|^2 + |\partial_x \psi|^2 - |\partial_y \psi|^2 - |\partial_z \psi|^2 \right)$$

$$E_{yy} = \frac{\rho_0}{2} \left(\frac{1}{c^2} |\partial_t \psi|^2 - |\partial_x \psi|^2 + |\partial_y \psi|^2 - |\partial_z \psi|^2 \right)$$

$$E_{zz} = \frac{\rho_0}{2} \left(\frac{1}{c^2} |\partial_t \psi|^2 - |\partial_x \psi|^2 - |\partial_y \psi|^2 + |\partial_z \psi|^2 \right)$$

$$E_{xy} = \rho_0 \partial_x \psi \partial_y \psi$$

$$E_{xz} = \rho_0 \partial_x \psi \partial_z \psi$$

$$E_{yz} = \rho_0 \partial_y \psi \partial_z \psi$$

51 where ρ_0 is the steady-state density of air and c the speed of sound.

52 In the specific cases of long enclosures (Dujourdy *et al.*, 2017) and flat spaces (Dujourdy

53 *et al.*, 2019), Dujourdy *et al.* were able to reduce the conservation of the stress-energy tensor

54 (eq. 1) to the telegraphers equation:

$$\frac{1}{c^2} \partial_{tt} E - \partial_{xx} E + \frac{A+D}{\lambda c} \partial_t E + \frac{AD}{\lambda^2} E = 0 \quad (2)$$

55 where E is the total energy, λ is the mean free path of the enclosure, and A and D are
 56 respectively modified absorption and scattering coefficients at the boundaries. Eq. (2) is
 57 symmetrical with respect to the absorption and scattering coefficients, as was confirmed by
 58 Meacham *et al.* (Meacham *et al.*, 2019) who systematically explored the whole space of values
 59 for the absorption and scattering coefficients and compared thus obtained reverberation
 60 times and spatial decays with the measured ones in a hallway. As shown in Fig. 1, the
 61 measured reverberation times and spatial decays correspond to narrow stripes of values for
 62 A and D , which do not always overlap; but most striking in Fig. 1 is the symmetry of the
 63 figure with respect to absorption and scattering coefficients. Physical justification of this
 64 symmetry is therefore the goal of the present paper.

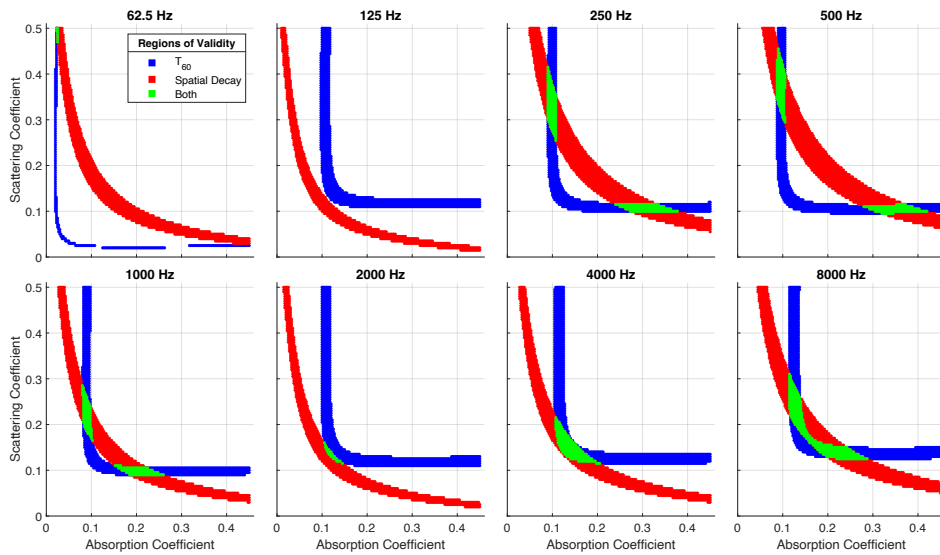


FIG. 1. Relevant combinations of absorption and scattering coefficients leading to measured reverberation times and spatial decays in a hallway (reproduced from (Meacham *et al.*, 2019)).

65 **III. WALL ADMITTANCE**

66 Now, wall admittance introduces a relation between the normal derivative and the time
 67 derivative of the velocity potential on the wall:

$$-\partial_n \psi = \frac{\beta}{c} \partial_t \psi = \frac{1}{c\zeta} \partial_t \psi$$

68 with \vec{n} the exterior normal to the wall, ζ the specific acoustic impedance of the wall ([Morse](#)
 69 [and Ingard, 1968](#), p. 580), that is, the wall impedance normalized by the characteristic
 70 impedance $\rho_0 c$ of air, and $\beta = \frac{1}{\zeta}$ is the specific acoustic admittance. Let us then consider
 71 a flat enclosure with vertical coordinate z . We can express the elements $E_{\cdot z}$ of the stress-
 72 energy tensor, where \cdot takes the values $t, x, \text{ or } y$. However, the admittance formalism implies
 73 a complex velocity potential, whereas the elements of the stress-energy tensor must remain
 74 real, as is expected from energy quantities. Thus, the expression for the non-diagonal terms
 75 of the stress-energy tensor must be modified as:

$$E_{tx} = -\frac{\rho_0}{c} \Re(\partial_t \psi \partial_x \psi^*)$$

$$E_{ty} = -\frac{\rho_0}{c} \Re(\partial_t \psi \partial_y \psi^*)$$

$$E_{tz} = -\frac{\rho_0}{c} \Re(\partial_t \psi \partial_z \psi^*)$$

$$E_{xy} = \rho_0 \Re(\partial_x \psi \partial_y \psi^*)$$

$$E_{xz} = \rho_0 \Re(\partial_x \psi \partial_z \psi^*)$$

$$E_{yz} = \rho_0 \Re(\partial_y \psi \partial_z \psi^*)$$

76 where the exponent $*$ means complex conjugated.

77 We thus obtain on the "ceiling":

$$\begin{aligned}
 E_{tz} &= \frac{\rho_0}{c^2} \Re(\partial_t \psi \beta^* \partial_t \psi^*) = \frac{\rho_0}{c^2} \Re(\beta) |\partial_t \psi|^2 \\
 E_{xz} &= -\frac{\rho_0}{c} \Re(\partial_x \psi \beta^* \partial_t \psi^*) = \Re(\beta) E_{tx} + \Im(\beta) \Im\left(\frac{\rho_0}{c} \partial_x \psi \partial_t \psi^*\right) \\
 E_{yz} &= -\frac{\rho_0}{c} \Re(\partial_y \psi \beta^* \partial_t \psi^*) = \Re(\beta) E_{ty} + \Im(\beta) \Im\left(\frac{\rho_0}{c} \partial_y \psi \partial_t \psi^*\right)
 \end{aligned} \tag{3}$$

78 and the same equations with opposite sign on the "floor". Note that E_{xz} and E_{yz} correspond
 79 to the parallel components of the radiation pressure exerted on the "ceiling" and the "floor"
 80 ([Stanzial *et al.*, 2002](#)).

81 IV. INTERPRETATION

82 Recalling that E_{tx} and E_{ty} are the components of the sound intensity in the x and
 83 y directions, we observe that the boundary conditions for E_{xz} and E_{yz} involve not only
 84 the active intensity associated with the real part of the admittance, but also the reactive
 85 intensity associated with the imaginary part of the admittance. This is not surprising, as
 86 the reactive intensity corresponds to local recirculation of energy, just as the imaginary part
 87 of the wall admittance is associated with a non-flat surface. Both phenomena contribute to
 88 the scattering of the impinging waves.

89 However, recalling that admittances are defined for pure waves only, we can further sim-
 90 plify these expressions by considering the phase angles ϕ_x and ϕ_y between the space deriva-
 91 tives of the velocity potential with respect to x and y respectively, and its time derivative.

92 The last two ceiling equations then reduce to:

$$E_{xz} = [\Re(\beta) + \Im(\beta) \tan \phi_x] E_{tx}$$

$$E_{yz} = [\Re(\beta) + \Im(\beta) \tan \phi_y] E_{ty}$$

93 As for E_{tz} , we must first express E_{tt} as a function of the wall admittance, that is:

$$\begin{aligned} E_{tt} &= \frac{\rho_0}{2} \left(\frac{1}{c^2} |\partial_t \psi|^2 + |\vec{\nabla} \psi|^2 \right) \\ &= \frac{\rho_0}{2} \left(\frac{1}{c^2} |\partial_t \psi|^2 + |\partial_x \psi|^2 + |\partial_y \psi|^2 + |\partial_z \psi|^2 \right) \\ &= \frac{\rho_0}{2} \left(\frac{1}{c^2} |\partial_t \psi|^2 + |\partial_x \psi|^2 + |\partial_y \psi|^2 + \left| \frac{\beta}{c} \partial_t \psi \right|^2 \right) \\ &= \frac{\rho_0}{2} \left(\frac{1}{c^2} [1 + |\beta|^2] |\partial_t \psi|^2 + |\partial_x \psi|^2 + |\partial_y \psi|^2 \right) \end{aligned}$$

94 Introducing the angle of incidence θ of the wave makes it possible to express the last two

95 terms in the previous equation as:

$$|\partial_x \psi|^2 + |\partial_y \psi|^2 = \frac{\sin^2 \theta}{c^2} |\partial_t \psi|^2$$

96 that is:

$$E_{tt} = \frac{\rho_0}{2c^2} (1 + \sin^2 \theta + |\beta|^2) |\partial_t \psi|^2 \quad (4)$$

97 leading to the following expression for the absorption coefficient:

$$\alpha(\theta) = \frac{E_{tz}}{E_{tt}} = \frac{2 \Re(\beta)}{1 + \sin^2 \theta + |\beta|^2} \quad (5)$$

98 The interpretations of the scattering coefficients D_x and D_y are similar. We simply

99 obtain:

$$D_x = \frac{E_{xz}}{E_{tx}} = [\Re(\beta) + \Im(\beta) \tan \phi_x] \quad (6)$$

$$D_y = \frac{E_{yz}}{E_{ty}} = [\Re(\beta) + \Im(\beta) \tan \phi_y]$$

100 **V. BOUNDARY CONDITIONS**

101 The evaluation of eqs. (6) takes different forms depending on the type of boundary and
 102 the position of the source.

103 **A. Plane wave on flat boundary**

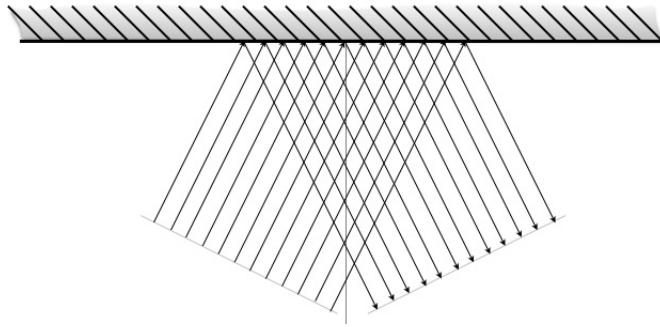


FIG. 2. Plane wave reflecting on flat boundary.

104 For a plane wave impinging on a flat boundary $z = 0$ (Fig. 2), the velocity potential
 105 takes the following form:

$$\psi(t, r) = \exp -i(\omega t - k_x x - k_y y - k_z z) + R \exp -i(\omega t - k_x x - k_y y + k_z z) \quad (7)$$

106 where ω is the radian frequency, k_x , k_y and k_z the components of the wave number $k = \frac{\omega}{c}$
 107 along the three coordinates, and R the complex reflection coefficient on the boundary. The
 108 first term in eq. (7) represents the impinging wave; and the second the reflected wave. The
 109 time derivative in the neighbourhood of the boundary is given by:

$$\partial_t \psi = -i\omega \psi = -i\omega \exp -i(\omega t - k_x x - k_y y) [\exp ik_z z + R \exp -ik_z z]$$

110 and the space derivatives by:

$$\begin{aligned}\partial_x \psi &= ik_x \psi = ik_x \exp -i(\omega t - k_x x - k_y y) [\exp ik_z z + R \exp -ik_z z] = -\frac{k_x}{\omega} \partial_t \psi \\ \partial_y \psi &= ik_y \psi = ik_y \exp -i(\omega t - k_x x - k_y y) [\exp ik_z z + R \exp -ik_z z] = -\frac{k_y}{\omega} \partial_t \psi\end{aligned}\quad (8)$$

$$\partial_z \psi = ik_z \exp -i(\omega t - k_x x - k_y y) [\exp ik_z z - R \exp -ik_z z] = -\frac{\beta}{c} \partial_t \psi$$

111 As a consequence, on the boundary $z = 0$, the phase angles ϕ_x and ϕ_y between the space
112 derivatives of the velocity potential with respect to x and y and its time derivative are both
113 equal to 0. In this case, eqs. (6) simply reduce to:

$$D_x = D_y = \Re(\beta)$$

114 that is, the scattering coefficient is purely created by absorption. Note that the last line
115 of eq. (8), together with the relation between the normal component of the wave number
116 and the angle of incidence $k_z = k \cos \theta = \frac{\omega}{c} \cos \theta$, gives the expected relation between the
117 complex reflection coefficient and the admittance:

$$R = \frac{\cos \theta - \beta}{\cos \theta + \beta} = \frac{[\cos^2 \theta - |\beta|^2] - 2i \cos \theta \Im \beta}{\cos^2 \theta + 2 \cos \theta \Re \beta + |\beta|^2}$$

118 B. Source at finite distance from flat boundary

119 For a spherical wave impinging on a flat boundary (Fig. 3), the velocity potential takes
120 a different form:

$$\psi(t, r) = \frac{\exp -i(\omega t - kr)}{4\pi r} + R \frac{\exp -i(\omega t - kr')}{4\pi r'} \quad (9)$$

121 where R still is the complex reflection coefficient on the boundary, r the distance to the real
122 source S , and r' the distance to the virtual image source S' (see Fig. 3). The first term in eq.
123 (9) represents the impinging wave; and the second the reflected wave. The time derivative

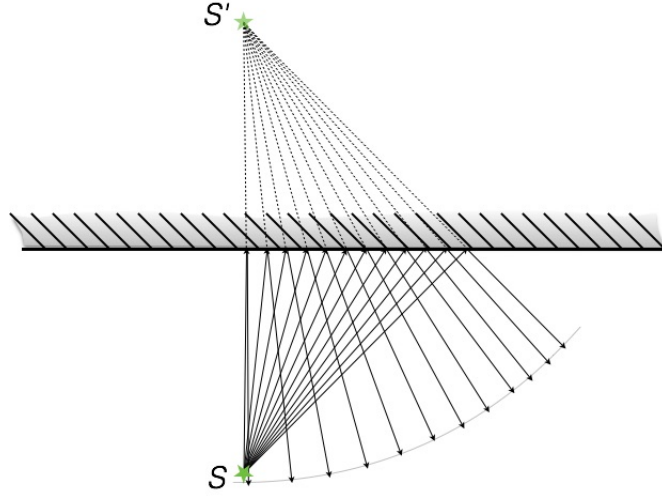


FIG. 3. Source at finite distance from flat boundary; S is real source, and S' virtual image source.

124 in the neighbourhood of the boundary is now given by:

$$\partial_t \psi = -i\omega \psi = -i\omega \frac{\exp -i\omega t}{4\pi} \left[\frac{\exp ikr}{r} + R \frac{\exp ikr'}{r'} \right] \quad (10)$$

125 and the space derivatives by:

$$\begin{aligned} \partial_x \psi &= i \frac{\exp -i\omega t}{4\pi} \left[k_x \frac{\exp ikr}{r} \left(1 + \frac{i}{kr} \right) + R k'_x \frac{\exp ikr'}{r'} \left(1 + \frac{i}{kr'} \right) \right] \\ \partial_y \psi &= i \frac{\exp -i\omega t}{4\pi} \left[k_y \frac{\exp ikr}{r} \left(1 + \frac{i}{kr} \right) + R k'_y \frac{\exp ikr'}{r'} \left(1 + \frac{i}{kr'} \right) \right] \\ \partial_z \psi &= i \frac{\exp -i\omega t}{4\pi} \left[k_z \frac{\exp ikr}{r} \left(1 + \frac{i}{kr} \right) + R k'_z \frac{\exp ikr'}{r'} \left(1 + \frac{i}{kr'} \right) \right] \end{aligned} \quad (11)$$

126 where k_x , k_y and k_z are the components of the incident wave number k along the three

127 coordinates, and k'_x , k'_y , and k'_z those of the reflected wave number k' . At the boundary, the

128 distance to the real and imaginary sources are equal, therefore $r = r'$; and $k_x = k'_x$, $k_y = k'_y$,

129 but $k'_z = -k_z$. The partial derivatives further reduce to:

$$\begin{aligned}
 \partial_t \psi &= -i\omega \frac{\exp -i(\omega t - kr)}{4\pi r} (1 + R) \\
 \partial_x \psi &= ik_x \frac{\exp -i(\omega t - kr)}{4\pi r} (1 + R) \left(1 + \frac{i}{kr}\right) = -\frac{k_x}{\omega} \left(1 + \frac{i}{kr}\right) \partial_t \psi \\
 \partial_y \psi &= ik_y \frac{\exp -i(\omega t - kr)}{4\pi r} (1 + R) \left(1 + \frac{i}{kr}\right) = -\frac{k_y}{\omega} \left(1 + \frac{i}{kr}\right) \partial_t \psi \\
 \partial_z \psi &= ik_z \frac{\exp -i(\omega t - kr)}{4\pi r} (1 - R) \left(1 + \frac{i}{kr}\right) = -\frac{\beta}{c} \partial_t \psi
 \end{aligned} \tag{12}$$

130 As a consequence, on the boundary, the phase angles ϕ_x and ϕ_y between the space derivatives
 131 of the velocity potential with respect to x and y and its time derivative are both equal to
 132 $\arctan \frac{1}{kr}$. And eqs. (6) reduce to:

$$D_x = D_y = \Re(\beta) + \frac{\Im(\beta)}{kr}$$

133 In this case, the imaginary part of the admittance contributes to the scattering coefficient,
 134 and this contribution is inversely proportional to kr . And according to the last line of eq.
 135 (12), the usual relation between the complex reflection coefficient and the admittance is
 136 modified into:

$$R = \frac{\cos \theta \left(1 + \frac{i}{kr}\right) - \beta}{\cos \theta \left(1 + \frac{i}{kr}\right) + \beta} = \frac{[\cos^2 \theta \left(1 + \frac{1}{k^2 r^2}\right) - |\beta|^2] - 2i \cos \theta \left[\Im \beta + \frac{\Re \beta}{kr}\right]}{\cos^2 \theta \left(1 + \frac{1}{k^2 r^2}\right) + 2 \cos \theta \left(\Re \beta + \frac{\Im \beta}{kr}\right) + |\beta|^2}$$

137 Note that this expression is equivalent to introducing a complex angle of incidence θ .

138 C. Curved boundary

139 In the case of a curved boundary, the real and virtual sources are not located at the
 140 same distance from the boundary (Fig. 4). As a consequence, eqs. (10) and (11) for the
 141 partial time and spaces derivative of the velocity potential are still valid in the vicinity
 142 of the boundary, provided that x , y and z are now considered as local coordinates at the

143 boundary, the two first ones being parallel to the boundary and the z one perpendicular
 144 to it. However, they do not simplify into eq. (12) at the boundary, even though $k_x = k'_x$,
 145 $k_y = k'_y$, and $k'_z = -k_z$, because $r' \neq r$.

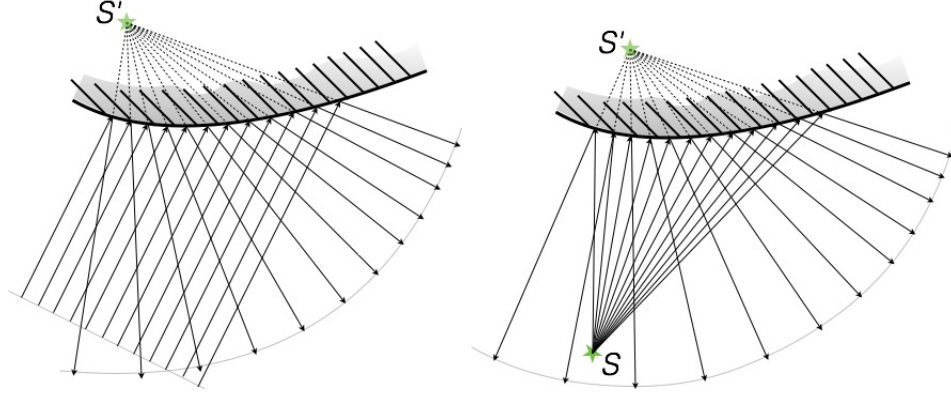


FIG. 4. Reflection on curved boundary. Left: plane wave impinging; right: source at finite distance. S is real source, and S' virtual image source.

146 On the boundary, we now obtain from eqs. (10) and (11):

$$\begin{aligned}\partial_x \psi &= -\frac{k_x}{\omega} \left(1 + i \frac{\frac{\exp ikr}{kr^2} + R \frac{\exp ikr'}{kr'^2}}{\frac{\exp ikr}{r} + R \frac{\exp ikr'}{r'}} \right) \partial_t \psi \\ \partial_y \psi &= -\frac{k_y}{\omega} \left(1 + i \frac{\frac{\exp ikr}{kr^2} + R \frac{\exp ikr'}{kr'^2}}{\frac{\exp ikr}{r} + R \frac{\exp ikr'}{r'}} \right) \partial_t \psi \\ \partial_z \psi &= -\frac{k_z}{\omega} \left(\frac{\left[\frac{\exp ikr}{r} - R \frac{\exp ikr'}{r'} \right] + i \left[\frac{\exp ikr}{kr^2} - R \frac{\exp ikr'}{kr'^2} \right]}{\frac{\exp ikr}{r} + R \frac{\exp ikr'}{r'}} \right) \partial_t \psi = -\frac{\beta}{c} \partial_t \psi\end{aligned}$$

147 where

$$\frac{\left[\frac{\exp ikr}{kr^2} + R \frac{\exp ikr'}{kr'^2} \right]}{\left[\frac{\exp ikr}{r} + R \frac{\exp ikr'}{r'} \right]} = \frac{\left[\frac{1}{kr^2} + \frac{R'}{kr'^2} \right]}{\left[\frac{1}{r} + \frac{R'}{r'} \right]} = \frac{1}{k} \frac{\frac{1}{r^3} + \left(\frac{1}{r} + \frac{1}{r'} \right) \frac{\Re(R')}{rr'} + \frac{|R'|^2}{r'^3} - i \left(\frac{1}{r} - \frac{1}{r'} \right) \frac{\Im(R')}{rr'}}{\frac{1}{r^2} + \frac{2\Re(R')}{rr'} + \frac{|R'|^2}{r'^2}}$$

148 with

$$\begin{aligned}
 R' = R \exp ik(r' - r) &= \frac{r' [\cos \theta (1 + \frac{i}{kr'}) - \beta]}{r [\cos \theta (1 + \frac{i}{kr'}) + \beta]} \\
 &= \frac{r' [\cos^2 \theta (1 + \frac{1}{k^2 r r'}) + \cos \theta \frac{\Im \beta}{k} (\frac{1}{r} - \frac{1}{r'}) - |\beta|^2]}{r [\cos^2 \theta (1 + \frac{1}{k^2 r'^2}) + 2 \cos \theta (\Re \beta + \frac{\Im \beta}{kr'}) + |\beta|^2]} \\
 &\quad + i \frac{r' \cos \theta [\frac{\cos \theta}{k} (\frac{1}{r} - \frac{1}{r'}) - 2 \Im \beta + \frac{\Re \beta}{k} (\frac{1}{r} + \frac{1}{r'})]}{r [\cos^2 \theta (1 + \frac{1}{k^2 r'^2}) + 2 \cos \theta (\Re \beta + \frac{\Im \beta}{kr'}) + |\beta|^2]} \quad (13)
 \end{aligned}$$

149 We then obtain:

$$\tan \phi_x = \tan \phi_y = \frac{1}{k} \frac{\frac{1}{r^3} + (\frac{1}{r} + \frac{1}{r'}) \frac{\Re(R')}{rr'} + \frac{|R'|^2}{r'^3}}{\frac{1}{r^2} + \frac{2\Re(R')}{rr'} + \frac{|R'|^2}{r'^2} + (\frac{1}{r} - \frac{1}{r'}) \frac{\Im(R')}{krr'}} \quad (14)$$

150 As a consequence, the phase angles ϕ_x and ϕ_y between the space derivatives of the velocity
 151 potential with respect to x and y and its time derivative are position dependent - and depend
 152 on the local angle of incidence θ - through the modified reflection coefficient R' . No simple
 153 equation subsists for eqs. (6) to reduce to.

154 Note that, in the case of a plane wave incident on a curved boundary (left pane of Fig.
 155 4), recalculating eqs. (13) and (14) gives the simpler formulas:

$$\begin{aligned}
 R' &= \frac{r' [\cos \theta - \beta]}{\cos \theta (1 + \frac{i}{kr'}) + \beta} = r' \frac{[\cos^2 \theta - \cos \theta \frac{\Im \beta}{kr'} - |\beta|^2] - i \cos \theta [\frac{\cos \theta}{kr'} + 2 \Im \beta - \frac{\Re \beta}{kr'}]}{\cos^2 \theta (1 + \frac{1}{k^2 r'^2}) + 2 \cos \theta (\Re \beta + \frac{\Im \beta}{kr'}) + |\beta|^2} \\
 \tan \phi_x = \tan \phi_y &= \frac{1}{kr'^2} \frac{\Re(R') + \frac{|R'|^2}{r'}}{1 + \frac{2\Re(R')}{r'} + \frac{|R'|^2}{r'^2} - \frac{\Im(R')}{kr'^2}}
 \end{aligned}$$

156 VI. DISCUSSION

157 A. Absorption coefficient

158 The form for the absorption coefficient given by eq. (5) does not reduce to the form
 159 given by Morse and Ingard (Morse and Ingard, 1968, p. 580) and introduced in acoustics

160 by Paris (Paris, 1927). However, but for a constant multiplicative factor, it is similar to
 161 an expression given by Bosquet (Bosquet, 1967). As Bosquet further explains, the form
 162 taken by the absorption coefficient strongly depends on the weighting function, that is, the
 163 statistics one chooses for computing the mean absorption coefficient. In the present case,
 164 the obvious choice is the so-called star-type statistics introduced by London (London, 1950),
 165 that is, taking the mean value of the equation $E_{tz} = \alpha E_{tt}$:

$$\int_0^{\frac{\pi}{2}} E_{tz} \sin \theta d\theta = \alpha^* \int_0^{\frac{\pi}{2}} E_{tt} \sin \theta d\theta \quad (15)$$

166 Compared to the more usual bar-type statistics (Bosquet, 1967; London, 1950), the star-type
 167 statistics does not include the factor $\cos \theta$; but there is no need to introduce this factor as
 168 E_{tz} already contains it, since it is the normal flux into the wall. Therefore is the star-type
 169 statistics the obvious choice. Assuming as usual an isotropic distribution of wave directions,
 170 the term $|\partial_t \psi|^2$ is then constant for all wave directions in the first line of eq. (3) and in eq.
 171 (4). The left hand side of eq. (15) simply reduces to the mean value of $\sin \theta$; and the right
 172 hand side also includes the mean value of $\sin^3 \theta$. Therefore, one obtains:

$$\alpha^* = \frac{2 \Re(\beta)}{1 + \frac{2}{3} + |\beta|^2} \quad (16)$$

173 which is the value of $\alpha(\theta)$ taken for $\theta = 55^\circ$, an angle that has repeatedly appeared since
 174 the 1950s as the incidence angle that represents the mean absorption (Bosquet, 1967; Guig-
 175 nouard, 1991; Vogel, 1956). Indeed, $\sin^2 55^\circ = 0.67 \approx \frac{2}{3}$.

176 Simple calculation shows that the absorption coefficients given by eq. (5) and (16) take
 177 values between 0 and a maximum reached when $\Re(\beta) = \sqrt{1 + \sin^2 \theta + \Im^2(\beta)}$ and $\Re(\beta) =$
 178 $\sqrt{1 + \frac{2}{3} + \Im^2(\beta)}$ respectively. This maximum is respectively equal to $\frac{1}{\sqrt{1 + \sin^2 \theta + \Im^2(\beta)}}$ and

179 $\frac{1}{\sqrt{1+\frac{2}{3}+\Im^2(\beta)}}$, that is, reaches its absolute maximum for $\Im(\beta) = 0$ with value $\frac{1}{\sqrt{1+\sin^2\theta}}$ and
 180 $\frac{1}{\sqrt{1+\frac{2}{3}}} \approx 0.775$ respectively. Both absolute maxima are therefore smaller than 1, except at
 181 normal incidence ($\theta = 0$) for the first one.

182 Last but not least, integrating eq. (16) on octave or third octave energy bands leads to
 183 the usual definition of band related absorption coefficients.

184 B. Scattering coefficients

185 The scattering coefficients given by eq. (6) are independent of the incidence angle θ ,
 186 except through the reflection coefficient in the expression of $\tan\phi_x$ and $\tan\phi_y$ for curved
 187 boundaries. However, the real part of the wall admittance contributes to the scattering
 188 coefficients. In other words, absorption on the wall induces scattering. This is a novel
 189 result.

190 Also novel is the observation that scattering coefficients are not bounded: they can take
 191 any value between $-\infty$ and $+\infty$, as is easily seen from eq. (6).

192 Traditionally, scattering is considered as the result of two mechanisms (Embrecchts, 2002):
 193 finite dimensions of reflecting surfaces; and roughness of the reflecting surfaces. There is no
 194 doubt from Sect. VC that the second term of eq. (6) corresponds to scattering by surface
 195 roughness, since it is driven by the finite distance from the surface to the image source.
 196 However, this term subsists for sources located at finite distances from a flat reflecting
 197 surface (see Sect. VB), as long as its admittance admits an imaginary part. But roughness
 198 is usually associated with locally varying imaginary parts of the admittance, as can be easily

199 demonstrated with Schroeder diffusers, where the depths of the wells drive this imaginary
 200 part. In the present case, no locally varying admittance is necessary to induce scattering.

201 We therefore suspect that the mechanism described in Sect. V does not correspond
 202 to traditional scattering, but to a different effect. Indeed, in the work of Dujourdy *et al.*
 203 (Dujourdy *et al.*, 2017, 2019) and Meacham *et al.* (Meacham *et al.*, 2019), the scattering
 204 coefficient induces a decrease of steady-state energy with distance. Although scattering does
 205 induce a decrease of steady-state energy with distance by redirecting part of it toward the
 206 source, no redirection is here at stake, just a reduction of the acoustical intensity by friction
 207 on the walls. In other words, total energy and acoustical intensity can be considered as
 208 two coupled systems that each follow its own conservation equation with some exchange
 209 between the two systems. As is well known from such coupled systems, the less damped
 210 system drives the energy decay with time, which precisely is what is obtained in Fig. 1.

211 As a consequence, the scattering coefficient D is ill-named. A better designation would
 212 be *intensity-friction* coefficient, or simply *friction* coefficient. For the time being, we stick
 213 to usage and keep the designation "scattering coefficient".

214 Note that, as for the absorption coefficient, integrating eq. (6) on octave or third octave
 215 energy bands leads to band related scattering - or friction - coefficients.

216 C. Admittance, impedance, and acoustic resistance

217 From the expression of the absorption and scattering coefficients (eqs. 5 and 6), it becomes
 218 possible to express the specific acoustic admittance in the case of flat walls, which is the case

219 of Fig. 1. From this expression, the specific acoustic impedance and the acoustic resistance
 220 of the wall can also be computed.

221 Table I presents the value of the octave-band absorption and scattering coefficients of
 222 the hallway of Fig. 1, derived from the figure itself by taking the centre of the vertical
 223 green patches. There is no green patch in Fig. 1 for the 125 Hz octave band, but the two
 224 stripes are tangent to each other at the point used in Table I. Note that, according to eq.
 225 (6), the real part of the specific acoustic admittance is equal to the scattering coefficient
 226 (plane walls). The imaginary part is obtained from eq. (5) which gives valid values for all
 227 octave bands. Two possibilities exist here: either considering a diffuse sound field, and use
 228 the average absorption coefficient of eq. (16); or considering that the sound field remains
 229 parallel to the walls, and use eq. (5) with $\sin \theta = 0$. The latter case gave more consistent
 230 results.

231 The specific acoustic impedance is then computed as the inverse of the specific acoustic
 232 admittance, and multiplying its real part by the characteristic impedance of air $\rho_0 c = 410$
 233 Ns/m^3 approximates the acoustic resistance of the wall - also in Ns/m^3 . No attempt has
 234 been made to compare the obtained values to typical walls, given that they are made of
 235 particle boards and gyps boards, with a hard plastic floor. Indeed, quick evaluation of
 236 the resonances of the walls by knocking on them revealed a complex structure with many
 237 resonances spread over all the octave bands of interest, rendering inconsistent the parsing
 238 of the measured impedance into resonances.

TABLE I. Admittance, impedance and acoustic resistance of the walls of the hallway of Fig. 1.

octave band	63Hz	125Hz	250Hz	500Hz	1kHz	2kHz	4kHz	8kHz
absorption coeff.	0.025	0.115	0.1	0.095	0.09	0.12	0.14	0.13
scattering coeff.	0.6	0.125	0.335	0.355	0.22	0.135	0.145	0.23
$\Re(\beta)$	0.6	0.125	0.335	0.355	0.22	0.135	0.145	0.23
$\Im(\beta)$	6.83	1.08	2.036	2.52	1.96	1.11	1.02	1.58
$\Re(\zeta)$	0.013	0.106	0.059	0.055	0.057	0.108	0.135	0.091
$\Im(\zeta)$	-0.15	-0.92	-0.41	-0.39	-0.50	-0.89	-0.96	-0.62
resistance (Ns/m^3)	5.23	43.7	24.1	22.5	23.2	44.3	55.5	37.1

239 VII. CONCLUSION

240 Starting with the precedent papers of Dujourdy *et al.* (Dujourdy *et al.*, 2017, 2019)
241 that have shown that integrating the stress-energy tensor in a disproportionate enclosure
242 and taking into account the boundary conditions leads to "loss terms" that correspond to
243 absorption and scattering, we expressed the elements of the stress-energy tensor with the
244 help of the wall admittance relation between normal derivative and time derivative of the
245 velocity potential on the wall.

246 As expected, the absorption coefficients are proportional to the real part of the wall
247 admittance. However, they also depend on the angle of incidence of the wave, leading to an
248 expression of the absorption coefficient eq. (16) which has been signaled in the literature,

249 for example by Bosquet (Bosquet, 1967), yet is not very usual; and to scattering coefficients
250 additively involving the real and imaginary parts of the wall admittance, as seen in eq.
251 (6), proving the absorptive nature of the scattering coefficient in the stress-energy tensor
252 formalism.

253 In the case of plane boundaries, calculations can be extended to evaluate the mean
254 impedance of the walls. An example is given for a long hallway.

255 ACKNOWLEDGMENTS

256 AUTHOR DECLARATIONS

257 Conflict of Interest

258 The authors have no conflicts to disclose.

259 Data Availability

260 Data sharing not applicable – no new data generated.

261

262 Bosquet, J. (1967). “La théorie synthétique de la réverbération,” in *Bulletin du Laboratoire*
263 *d’Acoustique de l’Université de Liège 11*, pp. 51–67.

264 Dujourdy, H., Pialot, B., Toulemonde, T., and Polack, J.-D. (2017). “Energetic wave equa-
265 tion for modelling diffuse sound field - Applications to corridors,” *Acta Acust united Ac*

266 **103**(3), 480–491.

267 Dujourdy, H., Pialot, B., Toulemonde, T., and Polack, J.-D. (2019). “Energetic wave equa-
 268 tion for modelling diffuse sound field - Applications to open offices,” *Wave Motion* **87**,
 269 193–212.

270 Embrechts, J.-J. (2002). “Modélisation des réflexions diffuses en acoustique des salles : état
 271 de la question,” in *6ème Congrès Français d’Acoustique*, pp. 666–669.

272 Guignouard, P. (1991). “L’absorption acoustique des matériaux poreux - prédictions et
 273 mesures,” Ph.D. thesis, Université du Maine.

274 London, A. (1950). “The determination of reverberant sound absorption coefficients from
 275 acoustic impedance measurements,” *J. Acoust. Soc. Am.* **22**(2), 263–269.

276 Mann, J., Tichy, J., and Romano, A. (1987). “Instantaneous and time-averaged energy
 277 transfer in acoustic fields,” *J. Acoust. Soc. Am.* **82**(1), 17–30.

278 Meacham, A., Badeau, R., and Polack, J. D. (2019). “Lower bound on frequency validity
 279 of energy-stress tensor based diffuse sound field model,” in *23rd International Congress on*
 280 *Acoustics*.

281 Morse, P. M., and Feshbach, H. (1956). *Mathematical Methods of Theoretical Physics* (Mc
 282 Graw-Hill Book Company).

283 Morse, P. M., and Ingard, K. U. (1968). *Theoretical Acoustics* (Mc Graw-Hill Book Com-
 284 pany).

285 Ollendorff, F. (1969). “Statistical room acoustics as a problem of diffusion, a proposal,”
 286 *Acustica* **21**, 236–245.

- 287 Paris, E. T. (1927). “On the reflexion of sound from a porous surface,” Proc. R. Soc. Lond.
288 A **115**, 407–419.
- 289 Picaut, J., Simon, L., and Polack, J. D. (1997). “A mathematical model of diffuse sound
290 field based on a diffusion equation,” Acta Acust. united Ac **83**(4), 614–621, [http://www.
291 ingentaconnect.com/content/dav/aaau/1997/00000083/00000004/art00006](http://www.ingentaconnect.com/content/dav/aaau/1997/00000083/00000004/art00006).
- 292 Polack, J. (2023). “Energy relationships in enclosures,” in *forum acusticum 2023*.
- 293 Stanzial, D., Bonsi, D., and Schiffrer, G. (2002). “Four dimensional treatment of linear
294 acoustic fields and radiation pressure,” Acta Acust. united Ac. **89**(2), 213—224, [https:
295 //www.ingentaconnect.com/content/dav/aaau/2003/00000089/00000002/art00002](https://www.ingentaconnect.com/content/dav/aaau/2003/00000089/00000002/art00002).
- 296 Stanzial, D., and Graffigna, C. E. (2017). “On the general connection between wave
297 impedance and complex sound intensity,” Proc. Mtgs. Acoust. **30**(1), 055013, [https:
298 //doi.org/10.1121/2.0000797](https://doi.org/10.1121/2.0000797).
- 299 Stanzial, D., and Schiffrer, G. (2010). “On the connection between energy velocity, re-
300 verberation time and angular momentum,” J. Sound Vib. **329**(7), 931–943, [https:
301 //doi.org/10.1016/j.jsv.2009.10.011](https://doi.org/10.1016/j.jsv.2009.10.011).
- 302 Vogel, T. (1956). “Sur les propriétés acoustiques des matériaux,” L’Onde Electrique **36**,
303 428–434.